Available online at www.sciencedirect.com
SCIENCE DIRECT®
Physica B 356 (2005) 51–55
PHYSICA B
www.elsevier.com/locate/physb

Grazing incidence neutron diffraction from ferromagnetic films in multi-domain state

B.P. Toperverg[a,b], V.V. Lauter-Pasyuk[c,d,*], H.J. Lauter[a], A. Vorobiev[a,b,e]

[a]*Institut Laue Langevin, B.P. 156, Grenoble 38000, France*
[b]*Petersburg Nuclear Physics Institute, 188300 Gatchina, St. Petersburg, Russia*
[c]*TU München, Physics Department, D-85747 Garching, Germany*
[d]*Joint Institute for Nuclear Research, Dubna, Moscow Region, Russia*
[e]*Max-Planck-Institut für Metallforschung, Stuttgart, D-70569, Germany*

Abstract

Bragg diffraction at grazing incidence of neutrons from a magnetic film decomposed into a set of ferromagnetic domains is considered within the frame of the distorted wave Born approximation. It is shown that the diffracted intensity measured as a function of angles of incidence and exit in the direction normal to the surface can provide information on the lateral distribution of domain magnetization. Theoretical results are illustrated by measurements of a mono-crystalline film of iron.

PACS: 1.12.Ha; 75.60.Ej; 75.75.+a

Keywords: Neutron reflectometry; Grazing incidence diffraction

Despite the fact that neutron diffraction at grazing incidence (GIND) was observed [1,2] a long time ago, it still remains a rather exotic method rarely applied to investigate atomic scale magnetic structures of thin films. This is in drastic contrast with a routine use of X-ray diffraction in studies of crystalline structures, as well as with polarized neutron reflectometry (PNR) commonly employed [3,4] to gain magnetization depth profiles across magnetic films and multi-layers. Neutron scattering in off-specular directions (OSNS) measured in addition to PNR provide rather valuable information on the lateral distribution of magnetization [3], in particular, due to magnetic domains. A reason of the restricted use of GIND is relatively low luminosity of the method, which therefore requires a careful choice of the subject adequate to capabilities of the method.

*Corresponding author. Institute Laue Langevin, B.P. 156, Grenoble Cedex 9 38042, France. Tel.: +33 4 76 20 75 56; fax: +33 4 76 20 71 20.
E-mail address: vlauter@ill.fr (V.V. Lauter-Pasyuk).

0921-4526/$ - see front matter © 2004 Elsevier B.V. All rights reserved.
doi:10.1016/j.physb.2004.10.045

One of the most apparent advantages of GIND with respect to PNR and OSNS is attributed [2] to its sensitivity to the magnetic moment direction normal to the surface. This property is rather important for the investigation of systems with, for instance, perpendicular anisotropy. Here we, however, discuss another example which benefits from GIND, the system with the in-plane magnetization broken into a set of domains. In this case, an interpretation of the data of PNR crucially depends on the ratio between domain size and the lateral projection $l_{\|}$ of the coherence length l. If domains are large then each of them reflect independently, the measured signal at the specular position is interpreted as an incoherent sum of reflections from individual domains. In the case of small domains specular reflection is, on the contrary, due to the *mean* magnetization averaged over a scale greater than $l_{\|}$. In order to distinguish between these two limiting cases one needs a careful analysis of the lineshape of the scattered signal. If domains are large then the width of the reflected beam is mostly determined by the resolution of the instrument, while no OSNS should be recorded. In the opposite case the resolution limited peak of specular reflection from the *mean* optical potential is superimposed onto the *diffuse* OSNS caused by magnetization fluctuations around this mean value. Very often, however, neither of the two asymptotic conditions is fulfilled, and if the domain size is comparable with the coherence length then the lineshape of the reflected beam may be substantially distorted. This would not allow to unambiguously separate specular reflection and off-specular scattering. Then one is faced with a severe problem of the quantitative analysis of PNR data, while GIND is free of this disadvantage.

Coherence properties of the beam in reflectometry are mostly determined by the collimation. Usually the uncertainty $\Delta\alpha$ in angles of incidence (reflection) α is small, while the resolution $\Delta\chi$ in azimuthal angle χ within the surface plane is quite relaxed. Therefore, the degree of the beam coherency is rather anisotropic. A coherence length projection across the film, i.e. transverse coherence length $l_{\perp}$ is estimated as $l_{\perp} \sim \lambda/(\Delta\alpha)$, where λ is the wavelength and $\Delta\alpha$ is an uncertainty in α. Coherence is also anisotropic within the film surface, even at the point-like collimation, e.g. at $\Delta\alpha \approx \Delta\chi$. Indeed, along the trace of the incoming beam on the surface it can be estimated as $l_{\|} \sim \lambda/(\alpha\Delta\alpha)$, while in the direction normal the reflection plane $l_{\chi} \sim \lambda/\Delta\chi \ll l_{\|}$. Due to this anisotropy the coherence volume in reflection kinematics is actually represented by a rather narrow bar substantially elongated along the line of intersection of the reflection plane and the surface, while with the shortest dimension across this plane. In this direction l_{χ} usually does not exceed a few hundreds of Ångstrøm and is much smaller than the domain size. On the contrary, $l_{\|}$ can cover a few dozens of micrometers, a scale greater, or comparable with the size of domains. In the latter case the averaging procedure in PNR may become rather uncertain. Indeed, if $l_{\|}$ crosses only a very few domains, then fluctuations around mean potential may become comparable with its mean value. Then they cannot be accounted for as a perturbation and quantitative analysis of PNR data becomes nearly impossible.

The situations with GIND is qualitatively different due to the fact that the coherence volume for the atomic scale diffraction is much smaller than for reflectivity. Indeed, GIND implies that the azimuthal Bragg angle χ_B is large: $\sin\chi_B = \lambda/2a$, where a is the unit cell constant. The coherence range determined by the resolution includes not only uncertainty of the incoming beam, but also the uncertainty in the angles of detection. As a result, the coherence range of GIND can be estimated as the area of intersection of two narrow bars: the one is that described above and the other rotated for the angle χ_B around normal to the surface. As a result, the coherence length for GIND reduces in any direction down to the value of the order $\lambda/(\Delta\chi)$ which is much smaller than characteristic size of ferromagnetic domains. This means that GIND is a sort of a local probe for domain magnetization: diffraction intensity calculated for each single domain is to be just added incoherently.

This procedure differs from that used to describe off-specular scattering from a multidomain state [3]. However, the general recipe of the distorted wave Born approximation (DWBA)

applies if the total diffracted intensity is small compared with either the incident on the sample, or the one specularly reflected. In contrast to DWBA developed [5] for OSNS it accounts exactly for the optical effects from the mean optical potential averaged over atomic structure inside domains, while deviations from this mean value due to the crystalline magnetic (and nuclear) structure is treated as a perturbation. The periodic perturbation adds to the lateral projection $\boldsymbol{\kappa}_i$ of the incident wave vector $\boldsymbol{k}_i$ a reciprocal lattice vector $\boldsymbol{\tau}$ so that the lateral projection of outgoing wave vector $\boldsymbol{k}_f$ is $\boldsymbol{\kappa}_f = \boldsymbol{\kappa}_i + \boldsymbol{\tau}$ (see sketch in Fig. 1).

The effect of the mean potential is birefringence of the neutron waves within a domain (see Fig. 1). The spin components of the neutron waves, either initial, or diffracted, propagate inside the domain with the wave vectors $\boldsymbol{k}^{\pm}_{i,f} = \{\boldsymbol{\kappa}_{i,f}; p^{\pm}_{i,f}\}$ split due to the Zeeman effect so that wave vector components normal to the surface complete a doublet $p^{\pm}_{i,f} = \sqrt{p^2_{i,f} - p^2_{c\pm}}$. Here $p_{i,f} = k \sin \alpha_{i,f}$, α_i is the incident, while α_f is outgoing angles, and $p_{c\pm}$ are critical wave numbers of the total reflections for positive and negative spin projections onto the domain magnetization direction $\boldsymbol{m} = \boldsymbol{M}/|\boldsymbol{M}|$. Inside each domain both the initial and diffracted waves are linear combinations of transmitted and reflected waves with transmission, $t^{\pm}_{i,f}$, and reflection, $r^{\pm}_{i,f}$, amplitudes corresponding to the signs of the neutron spin projections onto the unit vector $\boldsymbol{m}$. Therefore, in DWBA the scattering amplitudes are also represented as linear combinations of matrix elements of the diffraction potential enveloped with transmission and reflection amplitudes. The matrix elements can be expressed via the Born scattering amplitude operator $\hat{f}_B = \hat{f}_N + \hat{f}_M$, where $\hat{f}_N = f_N(\boldsymbol{Q})\hat{1}$, $\hat{f}_M = f_M(\boldsymbol{Q})(\boldsymbol{m}_\perp\hat{\boldsymbol{\sigma}})$, $f_N(\boldsymbol{Q})$ and $f_M(\boldsymbol{Q}) = -b_M F_M(\boldsymbol{Q})$ are the amplitudes of nuclear and magnetic scattering, respectively, b_M is the neutron scattering length, $F(\boldsymbol{Q})$ is the magnetic ion form factor (multiplied with the structure factor), $\hat{\boldsymbol{\sigma}}/2$ is the neutron spin operator, and $\boldsymbol{m}_\perp = \boldsymbol{m} - \boldsymbol{e}(\boldsymbol{em})$ is the component of the vector $\boldsymbol{m}$ orthogonal to the unit vector $\boldsymbol{e} = \boldsymbol{Q}/|\boldsymbol{Q}|$ pointing along the wave vector transfer $\boldsymbol{Q}$.

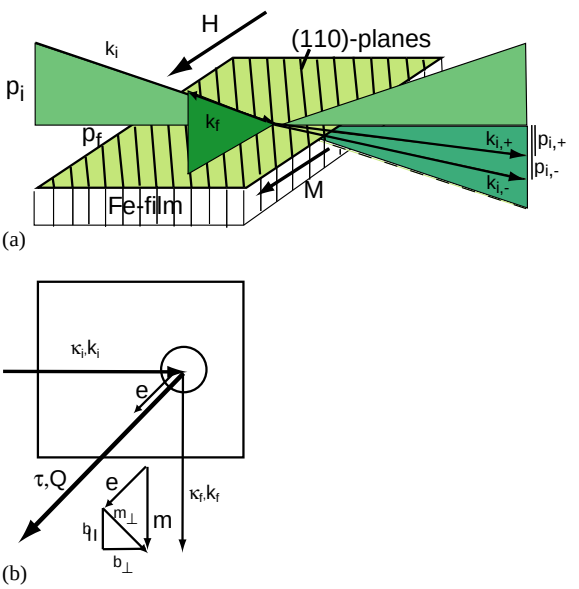

Fig. 1. GIND kinematics: (a) 3D view; (b) top view. The scattering angle of the (110) reflection is 85.6° and not 90°, as it is drawn in the figure for simplicity.

In view of DWBA it is convenient to decompose the vector $\boldsymbol{m}_\perp$ over two orthogonal vectors: $\boldsymbol{b}_\parallel = \boldsymbol{m}[1 - (\boldsymbol{em})^2]$ parallel and $\boldsymbol{b}_\perp = [\boldsymbol{m}(\boldsymbol{em}) - \boldsymbol{e}](\boldsymbol{em})$ orthogonal to $\boldsymbol{m}$. Then the amplitude of magnetic scattering $\hat{f}_M(\boldsymbol{Q}) = \hat{f}^{\parallel}(\boldsymbol{Q}) + \hat{f}^{\perp}(\boldsymbol{Q})$ is correspondingly decomposed into two terms. The first one, $\hat{f}^{\parallel}(\boldsymbol{Q})$, is diagonal with respect to the spin states if the quantization axis is chosen along with the vector $\boldsymbol{m}$. The second term, $\hat{f}^{\perp}(\boldsymbol{Q})$ is not diagonal and mixes neutron spin states.

At $\boldsymbol{Q} = 0$, i.e. in the homogeneous limit, the amplitude matrix $\hat{f}_B(0)$ is also diagonal and its eigenvalues $f_\pm(0) = f_N(0) \pm f_M(0)$ determine the optical constants $p^2_{c\pm} = 4\pi f_\pm(0)/v_0$, where v_0 is the unit cell volume. The scattering amplitude in the forward direction is accounted in exact calculations of the amplitudes of transmission, $a^t_\pm = t^\pm$, and amplitudes of reflection, $a^r_\pm = r^\pm$, as well as in the transverse projections of the four pairs of the wave number transfer $q^\pm_{tt} = p^\pm_f - p^\pm_i$, $q^\pm_{tr} = p^\pm_f + p^\pm_i$, $q^\pm_{rt} = -q^\pm_{tr}$, and $q^\pm_{rr} = -q^\pm_{tt}$. As a result the DWBA equation for the scattering cross section of unpolarized neutrons boils down to the following compact form:

$$\frac{d\sigma}{d\Omega} = \frac{1}{2}\sum_{\mu,\nu=+,-}\left|\sum_{\tau,\rho=t,r} a^{f\tau}_{\mu}\mathscr{F}^{\mu\nu}_{\tau\rho}a^{i\rho}_{\nu}\right|^2. \quad (1)$$

Here superscripts i, f refer to either incoming or outgoing neutron states, $\mathscr{F}^{\mu\nu}_{\tau\rho} = \mathscr{F}^{\mu\nu}(\boldsymbol{\tau}_\parallel)\mathscr{G}_\perp(q^{\tau\rho}_{\mu\nu})$, $\mathscr{F}^{\pm\pm}(\boldsymbol{\tau}_\parallel) = f_N(\boldsymbol{\tau}_\parallel) \pm f_M(\boldsymbol{\tau}_\parallel)[1-(\boldsymbol{em})^2]$, $|\mathscr{F}^{\pm\mp}(\boldsymbol{\tau}_\parallel)|^2 = |f_M(\boldsymbol{\tau}_\parallel)|^2(\boldsymbol{em})^2[1-(\boldsymbol{em})^2]$, the reciprocal lattice vector $\boldsymbol{\tau}_\parallel$ is displayed within the film surface plane, $\boldsymbol{e} = \boldsymbol{\tau}_\parallel/|\boldsymbol{\tau}_\parallel|$, and

$$\mathscr{G}_\perp(q) = \frac{\exp(\mathrm{i}qd) - 1}{\mathrm{i}qd} \tag{2}$$

is the transverse form factor of the film of the thickness d. In the case of multi-domain sample Eq. (1) should be averaged over the unit vectors $\boldsymbol{m}$ spread out in accordance with the domain magnetization distribution.

Eqs. (1) and (2) allow to express the DWBA scattering cross section via the bi-linear combination of the Born amplitudes $f_B(\boldsymbol{Q})$ decorated by the amplitudes of neutron waves transmitted into the film and reflected from the substrate. As a result the intensity distribution over the plane with the coordinates p_i and p_f reveal a rather rich in detail interference pattern, as seen in Fig. 2. The map is calculated for the diffraction reflex (1 1 0) for a 2500 Å thick Fe film deposited onto an MgO substrate. Calculations produced with a fine resolution show two rather strong peaks positioned at $p_i = p_f = p_{c\pm}$ and a pair of side peaks at $(p_i = p_{c+}, p_f = p_{c-})$ and $(p_i = p_{c-}, p_f = p_{c+})$. The first two correspond to the diffraction processes with no change in the neutron spin states, while the other two are due to the interference between spin states split in the mean magnetic field. The intensity of the latter reach maxima for diffraction from domains with magnetization directed at 45° with respect to $\boldsymbol{\tau}_\parallel$, while turns to zero if it is either parallel, or perpendicular to $\boldsymbol{\tau}_\parallel$. The fine oscillations in Fig. 2 are due to the sharp interfaces of the film which cause oscillations in amplitudes $t^\pm$ and $r^\pm$ as well as in the film form factors in Eq. (2). Those oscillations are smeared out due to the possible roughness of interfaces. However, at low angles $\alpha_{i,f}$ the most drastic effect is caused by the finite instrumental resolution. This effect is illustrated in Fig. 3 where the intensity in Fig. 2 is convoluted with the actual resolution of the reflecto-diffractometer EVA [6] at the ILL and compared with theexperimental results obtained on this instrument as shown in Fig. 4.

The sample of natural Fe was grown with molecular beam epitaxy on a MgO (1 0 0) substrate of a size of $20 \times 20\,\mathrm{mm}^2$. The experiment has been performed with an unpolarized beam with a wavelength of 2.75 Å. The sample was magnetized in a magnetic field of 50 Gs applied along the easy (1 0 0) direction, while intensity of the diffraction peak in the direction (1 1 0) was measured at a sequence of angles of incidence α_i. The signal was recorded over the linear position sensitive detector and recollected into the intensity map in Fig. 4, in which high-intensity manifests at $p_{c\pm} = 0.013$ and $0.007\,\mathrm{Å}^{-1}$, respectively. The positions of the peaks, as well as their intensities are well-described

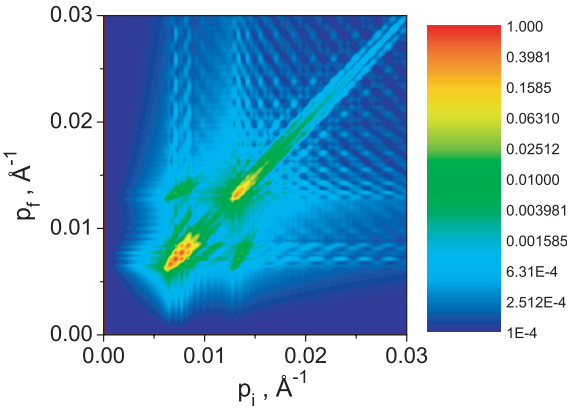

Fig. 2. Intensity distribution map for GIND from 2500 Å thick Fe film on MgO substrate calculated in accordance with Eqs. (1) and (2) with a fine resolution.

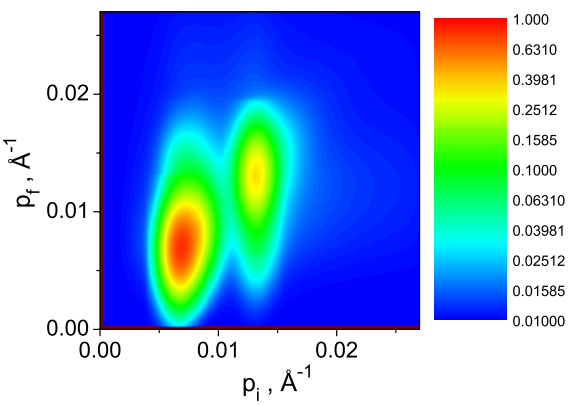

Fig. 3. The same intensity map as in Fig. 2 smeared over the actual resolution of the EVA reflecto-diffractometer.

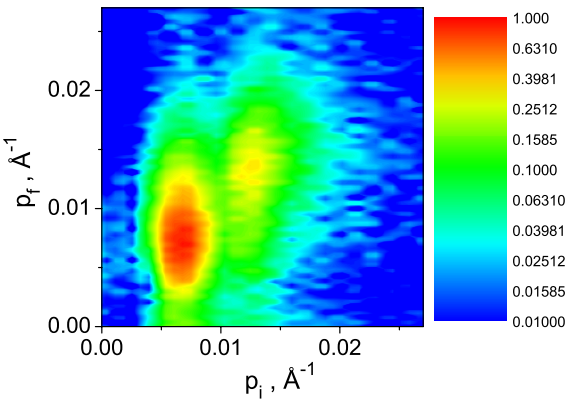

Fig. 4. Experimentally measured intensity distribution map for the same conditions as in Fig. 3.

theoretically and totally determined by in-domain magnetization. On the other hand, limited resolution of the instrument has not allowed to unambiguously separate side interference peaks. Therefore, we were not able to deduce from the present experiment the spread out of the domain magnetization directions in Fe film, which, is, however, expected to be small close to remanence.

Here, we demonstrated a feasibility of GIND to study multi-domain state in ferromagnetic films. The pilot experiment carried out on a Fe film has confirmed theoretical expectations and sufficient luminosity of the method. However, it also revealed the necessary improvements in the existing instrument dedicated for such studies, or requirements for new designed instruments of this type. The necessary improvement of resolution by a factor 2–3 can in principle be easily achieved at either ILL, or elsewhere.

Acknowledgements

We thank M. Milyaev, L. Romashov, V. Ustinov for providing us with the sample, E. Kats for fruitful discussions. The support of BMBF (Project 03DU03MU), Russian Ministry of Research (Contract 40.012.1.1.1149) and RFFI Grant (SS-1671.2003.2) are acknowledged.

References

[1] H. Dosch, Physica B 192 (1993) 163;
R. Günther, et al., Physica B 234 (1997) 508.
[2] R. Günther, W. Donner, B.P. Toperverg, H. Dosch, Phys. Rev. Lett. 81 (1998) 116.
[3] V. Lauter-Pasyuk, H.J. Lauter, B.P. Toperverg, L. Romashev, V. Ustinov, Phys. Rev. Lett. 89 (2002) 127203.
[4] S.G.E. te Velthuis, J.S. Jiang, S.D. Bader, G.P. Felcher, Phys. Rev. Lett. (2002).
[5] B.P. Toperverg, Physica B 279 (2001) 160;
B.P. Toperverg, Physica B 335 (2003) 174;
B.P. Toperverg, in: Polarized Neutron Scattering, Forschungszentrum Jülich, Series "Matter and Materials", vol. 12, 2002, p. 275.
[6] EVA, www.ill.fr.